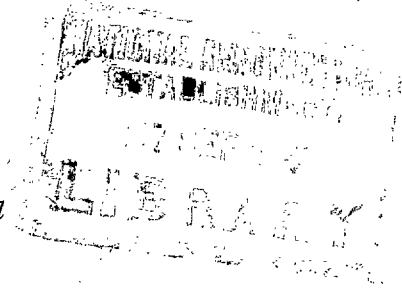# MINISTRY OF SUPPLY

AERONAUTICAL RESEARCH COUNCIL
REPORTS AND MEMORANDA

Tests on a Single-stage Turbine Comparing the Performance of Twisted with Untwisted Rotor Blades

By

I. H. JOHNSTON and L. R. KNIGHT

LONDON: HER MAJESTY'S STATIONERY OFFICE

1956

PRICE 3s 6d NET

Tests on a Single-stage Turbine Comparing the Performance of Twisted with Untwisted Rotor Blades

By

I. H. Johnston and L. R. Knight

Communicated by the Principal Director of Scientific Research (Air),
Ministry of Supply

Reports and Memoranda No. 2927[*]

February, 1953

Summary.—An experimental single-stage turbine designed for the testing of a variety of blade forms with cold air is described together with the instrumentation provided for test measurements.

Performance results obtained on this unit from two rotor blade designs are presented and it is shown that for the incidence range covered by the tests an untwisted constant-section blade of about 10 per cent reaction possesses characteristics of pressure loss and deflection nearly identical to those of a conventional rotor blade twisted along its length to conform to the requirements of radial equilibrium, the mean diameter sections of the two blade designs being identical. It should be noted that the rotor blade section used in these tests provides a gas outlet angle and degree of reaction which, although lower than those employed in current aircraft engine practice, may well become typical for designs requiring a higher volumetric flow per unit turbine frontal area, *e.g.*, a high temperature cooled turbine.

---

1. *Introduction.*—Up to the present time the task of relating the performance of a turbine to the many variables involved has been hindered by the lack of systemised test work. To meet this need a single-stage experimental turbine has been built which (while preserving geometrical similarity before and after the blade rows and with uniformity of instrumentation) can accommodate a wide variety of nozzle and rotor cascades. A description of this turbine and its accompanying instrumentation forms the first part of this memorandum.

The second part of the memorandum comprises the test results obtained from two rotor blade designs. These designs have a common mean diameter blade section but whereas the first design is conventional, *i.e.*, the blades have a radial twist to conform approximately to radial equilibrium conditions and are of varying section from root to tip, the second design consists of untwisted blades of constant section at all radii.

2. *General Arrangement of Test Rig.*—The layout of equipment in the test cubicle is illustrated in Fig. 1. The two main components are the turbine and the air brake. This brake consists of a single-sided centrifugal compressor with a row of variable-stagger swirl vanes located immediately before the eye of the impeller. By varying the degree of inlet swirl it is possible to obtain a limited range of power absorption at constant rotational speed. If required, further power control can be obtained from a throttle valve placed in the air inlet to the brake. The turbine torque is transmitted to the brake along a connecting shaft fitted at each end with gear-type couplings. The possibility of failure in power absorption due to either surging of the air brake or a mechanical failure makes it necessary to provide an overspeed trip gear. This gear automatically closes an emergency butterfly valve set in the main air supply line to the turbine, opens a blow-off valve located immediately upstream of the butterfly valve, and trips the main plant compressor.

A

All testing is done cold, *i.e.*, there is no combustion system and air is delivered to the turbine from the main supply at a temperature of approximately 100 to 120 deg. C.

Photographs of both air brake and turbine, together with details of the trip mechanism are published in Ref. 2.

3. *Description of Turbine*.—A simplified cross-sectional view of the turbine is shown in Fig. 2. The inlet volute is in the form of a massive scroll which encircles the turbine and from which the air passes to the inlet annulus via eight radial elbows. The high degree of acceleration imparted to the air by the volute results in uniform flow conditions at inlet to the turbine nozzle row. The nozzle blades are mounted on segmented rings which form the inner and outer annulus walls and are fitted as liners in the main casing. This type of construction simplifies the interchange of nozzle rows and permits of variation in axial spacing between rotor and stator. The bearing assembly is built into the centre of the volute casing and houses the turbine shaft on which is carried the overhung rotor disc. The shaft is held in two journal bearings, one of which is split to accommodate a Michell thrust bearing.

Three rotor discs are available for this turbine to accommodate varying numbers of rotor blades and, as with the nozzles, the interchange between rotors can be effected quickly and easily. Downstream of the rotor is the exhaust cone which is supported by spiders in the outlet pipe through which the air passes to atmosphere.

The turbine is supported on trunnion mountings set at either side of the volute on the horizontal centre line. A strut attached to the face of the turbine casing by a keyway locates the unit and allows for axial expansion ; a second keyway at the bottom of the volute prevents any transverse movement of the centre line.

As shown in Fig. 2 the inlet volute and turbine casing are lagged to minimize heat losses due to conduction and radiation.

4. *Instrumentation*.—Provision is made for the following measurements :

> Air mass flow
> Inlet total and static pressures
> Outlet total and static pressures
> Inlet total temperature
> Outlet total temperature
> Turbine r.p.m.
> Radial traverses of air angle and total pressure behind the rotor.

4.1. *Air Mass Flow*.—Measurement is by an orifice plate in a straight section of the inlet ducting. The orifice plate and static tappings are in accordance with the British Standard design specifications for flow measurements. Air temperature at the orifice plate is measured by a stagnation shielded thermocouple connected to a Cambridge indicator.

4.2. *Inlet Pressures*.—Total pressure is measured as the average from four pitot-tubes set at equal intervals round the mean diameter of the annulus upstream of the nozzle blades. These pitots were calibrated with respect to the area mean total pressure obtained by traversing the annulus with nozzle and rotor blades removed (*see* Ref. 3).

Static pressure was measured as a mean of four tappings around the outer wall of the annulus in the plane of the pitots.

4.3. *Outlet Pressures*.—Outlet total pressure is read by four five-point pitot-combs placed after the rotor. A rack and pinion mechanism provides for simultaneous yawing of the four combs, each of which carries an arrow-head yawmeter at mean diameter. For each reading the pitots at mean diameter can thus be accurately aligned with the direction of flow and for normal radial variations in air angle the pitots at other diameters are assumed to read total pressure. The pitots

are spaced radially on the combs to cover equal flow areas and thus an arithmetic mean of the five readings gives a true area mean value for total pressure after the turbine.

Static pressure is measured as a mean of four static tappings in both the outer and inner walls of the annulus.

4.4. *Temperature Measurement.*—As the construction of the air brake precludes accurate measurement of power by the standard dynamometer practice of weighing the torque reaction on the brake casing, the turbine work is calculated from the drop in total temperature of the air through the stage. Any error in this temperature drop is reflected directly in the efficiency estimation and so particular attention has been paid to the method of temperature measurement. Initial attempts to measure temperature with thermocouples placed immediately before and after the turbine blades led to a marked degree of scatter in the experimental results. Subsequent development has produced the present system which is described below.

Inlet temperature is measured by four thermocouples inserted in alternate elbows of the inlet volute. The couples being wired in series to give a single reading. Outlet air temperature is measured by eight thermocouples connected in two groups of four and covering two diameters in the outlet ducting downstream of the exhaust cone. The instruments are thus located in regions of comparatively low air velocity. Upstream of the outlet thermocouples a fine wire gauze is inserted to reduce radial variations in velocity, and behind this gauze is a honeycomb of straightener vanes designed to limit the swirl in the exhaust. The ducting is lagged to minimize heat loss due to conduction and radiation between the two measuring planes and the small remaining loss is calibrated out by passing air through the rig with both nozzle and rotor blades removed.

The thermocouples are of nichrome–constantan wire housed in stagnation shields. The cold junctions are threaded into a cylindrical bobbin covered with wax, and immersed in an ice flask. All voltage measurements are made on a potentiometer.

4.5. *Turbine r.p.m.*—Turbine rotational speed is measured with a Hasler tachometer, a Hasler point being provided at the rear of the air brake.

4.6. *Outlet Traverses.*—A traverse gear is fitted to the outlet casing in the plane of the outlet pitot combs. Traversing is limited to one radial line, but provides for measurement of air angle and total pressure at all radii from inside diameter to outside diameter.

5. *Test Results.*—5.1. *Blade Details.*—The nozzle blades used throughout the tests were of untwisted constant-section design. The conventional rotor blades were of impulse design at the root and were twisted to conform to the requirements of simple radial equilibrium and constant work done at all radii. For the rotational speed at which tests were carried out, namely $N/\sqrt{T} = 475$, the gas angles corresponding to zero incidence at the mean diameter section give a ' design ' value of $2gJk p \Delta T/U^2$ of $2\cdot5$ and a reaction of 10 per cent. The untwisted rotor blades had the same mean diameter section as the conventional blades and this section was preserved at all radii.

The blade profiles are shown in Fig. 3, and relevant details are tabulated below.

Nozzle blades			
Number of blades	36		
	Root	Mean	Tip
S/C	0·625	0·739	0·855
β_1	0°	0°	0°
β_2	−65°	−65°	−65°
O/S		0·437	
Chord (in.)	1·33	1·33	1·33

3

AI

Conventional rotor blades			
Number of blades	50		
	Root	Mean	Tip
S/C	0·597	0·744	0·906
β_1	47°	34°	21°
β_2	−46°	−52°	−60°
O/S (measured)	0·671	0·645	0·610
Chord (in.)	1·00	0·95	0·90
S/e		0·355	

Untwisted rotor blades			
Number of blades	50		
	Root	Mean	Tip
S/C	0·629	0·744	0·860
β_1	34°	34°	34°
β_2	−52°	−52°	−52°
O/S (measured)	0·640	0·655	0·661
Chord (in.)	0·95	0·95	0·95
S/e		0·355	

Rotor blades are unshrouded with a mean tip clearance of 0·040 in. Outer and inner annulus diameters are 13·0 in. and 9·5 in. respectively, giving a diameter ratio of 0·73 and a blade height of 1·75 in.

5.2. *Accuracy of Measurements.*—*Mass flow.*—Inlet conditions to the orifice plate were traversed and found to be uniform, and so the B.S.S. estimate of ± 0·75 per cent is accepted.

Temperature.—Samples of thermocouple wire were calibrated by the National Physical Laboratory and inaccuracies did not exceed 0·2 deg C. The potentiometer could be read accurately to within a voltage equivalent of 0·1 deg C.

Expressing these figures as percentages of the average turbine temperature drop, the absolute accuracy of ΔT (measured) lies within ± 1·2 per cent and the experimental scatter or relative accuracy may be taken as ± 0·4 per cent.

Pressure.—Errors in pressure readings are estimated to be not more than ± 2 per cent dynamic head.

Outlet air angle.—The traversing gear was calibrated for yaw on a calibrating tunnel to an accuracy of within ± ½ deg. This error was due to backlash in the gears and it can be largely eliminated by care in manipulation of the instrument.

5.3. *Constant Speed Characteristics.*—From mechanical considerations associated with the air brake the maximum rotational speed for these tests was limited to 10,000 r.p.m., and as at lower speeds the accuracy of the temperature drop measurement would be impaired, testing was limited to single line characteristics at an $N/\sqrt{T}$ of 475 (r.p.m. ≃ 9,500). A further restriction on the range of these tests was imposed by the surge point of the brake which limited the low load (negative incidence) side of the turbine characteristic.

The Reynolds number of the flow through the rotor varied from $1\cdot75 \times 10^5$ to $2\cdot85 \times 10^5$. Taking a critical value of R_e of $1\cdot0 \times 10^5$ (Ref. 2), the application of the test results to engine performance is unlikely to be impaired by any Reynolds number effect.

Results for the two rotors showing efficiency and mass flow plotted against pressure ratio are given in Fig. 4. The test points have a scatter of $\pm$ 1 per cent in efficiency and within the limit of this scatter there is negligible difference between the two rotors. The results for mass flow show even less scatter and again the two rotors give identical results.

Included in Fig. 4 are characteristics based on the mean diameter conditions and calculated according to the method detailed in Ref. 1. These show a peak efficiency of 88 per cent which is about $2\frac{1}{2}$ per cent below the test figure and a flow function which is about 3 per cent below the test curve. The discrepancy in efficiency may be partly explained by reference to the basic data used in the performance estimation. Rotor blade loss characteristics used in this method were derived from a variety of turbine tests in which power measurement was generally accomplished by the standard torque-weighing procedure. Unless detailed corrections are applied this method will tend to under-estimate blading efficiency as the power measurement will necessarily be diminished slightly by bearing friction and windage losses. In addition few practical turbine designs can provide inlet conditions which are comparable with those produced in the experimental rig. The differences between test and calculated mass flows suggest a discrepancy between actual and estimated flow areas, but discussion of this question is deferred to the following section.

5.4. *Traverse Results.*—Radial traverses of air outlet angle (α_3) and outlet total pressure were made at three points along the characteristic for each rotor. From these results and the nozzle traverses included in Ref. 3, the air angles relative to the rotors (α_1 and α_2) were calculated and radial distributions of these angles and the corresponding axial velocities (V_{a1} and V_{a2}) are shown in Figs. 5 and 6.

Considering first the results for the twisted rotor (Fig. 5), we see that the range of α_1, and hence the range of incidence covered by the traverses, is quite small. It is therefore not surprising that the values of α_2 remain almost unchanged over most of the blade height. Distribution (2) of α_1 corresponds to peak turbine efficiency (*see* Fig. 4) and comparing α_1 and β_1 we see that the mean incidence over the blade height for this condition approximates to zero.

The surprising feature of the air outlet angle distributions is the large discrepancy between α_2 (test) and α_2 estimated from $\cos^{-1} O/S$ and blade curvature (Ref. 1). To investigate this further a lengthened probe was used which advanced the plane of the traverse from one chord to $\frac{1}{5}$ chord behind the rotor trailing edge. No significant change in α_2 was detected. The air outlet angle estimated according to the method of Ref. 1 is strictly a momentum mean angle and the momentum mean of the test values of α_2 shows a discrepancy of 5 deg. As yet no reason for this unusually high deviation has been found but the normal explanation of deviation, namely stalling on the upper surface of the blade, would appear to be inadmissable in view of the high efficiency of the turbine and the low incidence range at inlet to the rotor. The end effects which are noticeable in the α_2 distributions can be attributed at the outside diameter to the tip clearance space and at the inside diameter to the boundary layer associated with the rotor disc. In the clearance space the air leaving the nozzles suffers only partial deflection and thus emerges with a low α_2, and near the inner wall it has been demonstrated (Ref. 4) that the pressure gradient across the boundary layer of the channel formed by adjacent blades induces secondary flow which results in a local increase in α_2 within the boundary layer.

Turning to the results for the untwisted rotor (Fig. 6) we see that at optimum efficiency although the mean incidence over the blade height again approximates to zero, the blade root is subject to a positive incidence of 10 deg and the tip to a negative incidence of nearly 20 deg. The similarity between the efficiencies obtained from the two rotors suggests that it is the conditions at mean diameter which are dictating blade loss coefficient and hence efficiency. The distributions of α_2 relative to the values for $\cos^{-1} O/S$ are very similar to those for the twisted

5

blades. The momentum mean angles are almost identical and the discrepancy between the measured outlet angle and the theoretical angle is virtually unchanged.

It should be noted that the values for $\cos^{-1} O/S$ and hence the estimated momentum mean outlet angles are based on actual measurements of blade opening made on the rotor assemblies.

The difference of 5 deg between estimated and measured air outlet angle suggested a possible explanation for the discrepancy between calculated and test $Q\sqrt{T}/P$. The performance estimate was therefore recalculated using the test values of momentum mean angle and the resultant flow characteristic is shown in Fig. 4. The improved agreement between this characteristic and the test values confirms the high measured deviation and indicates that for the blading tested some modification to the method for estimating α_2 is required.

5.5. *Characteristics in Terms of* $2gJkp\Delta T/U^2$.—In Fig. 7 the measured temperature drops for each rotor are related to incidence by plotting the stage work coefficient against V_a/U. The agreement between the results for the two rotors reflects the similarity in momentum mean outlet angle observed in the traverse results. Additional values of stage work based on the change of whirl of the air through the turbine computed from the traverse results are also shown and the agreement between the measured and calculated temperature drops is reassuring in view of the general suspicion with which temperature drop measurement in turbines is sometimes regarded.

6. *Conclusions*.—(*a*) A general description of a single-stage turbine test rig and the turbine instrumentation has been presented.

(*b*) Test results have been obtained which compare the performance of a conventional twisted rotor blade with that of a constant-section untwisted blade designed on the same mean diameter section.

(*c*) The results show that for the limited incidence range covered by the tests, the two rotors give identical characteristics.

(*Note*.—Any generalization of the above conclusion must strictly be limited to diameter ratios of 0·73 and above.)

4. Detailed investigation of the air flow after the rotors indicates that at least for the type of blades tested some further investigation into methods for estimating α_2 is desirable.

LIST OF SYMBOLS

C	Blade chord (in.)
e	Mean radius of curvature of the convex surface of a blade between the throat and the trailing edge (in.)
kp	Specific heat at constant pressure
O	Blade opening or throat (in.)
P	Total pressure (lb/sq in. abs.)
S	Blade pitch or spacing (in.)
T	Total gas temperature (deg K)
ΔT	Gas total temperature drop across turbine (deg C.)
U_m	Rotor blade speed at mean diameter (ft/sec)
V	Gas velocity (ft/sec)
V_a	Axial component of gas velocity (ft/sec)
Q	Gas mass flow (lb/sec)
α	Gas flow angle relative to axial direction
β	Blade angle relative to axial direction
η	Isentropic total-head efficiency

6

REFERENCES

No.	Author	Title, etc.
1	D. G. Ainley and G. C. R. Mathieson ..	A method of performance estimation for axial flow turbines. N.G.T.E. Report R.111. A.R.C. 14,882. (To be published.)
2	D. G. Ainley	The performance of axial flow turbines. *Proc. I.Mech.E.* Vol. 159. 1948.
3	I. H. Johnston	An analysis of the air flow through the nozzle blades of a single-stage turbine. C.P.131. February, 1951.
4	A. D. S. Carter	Three dimensional flow theories for axial compressors and turbines *Proc. I.Mech.E.* Vol. 159. 1948.
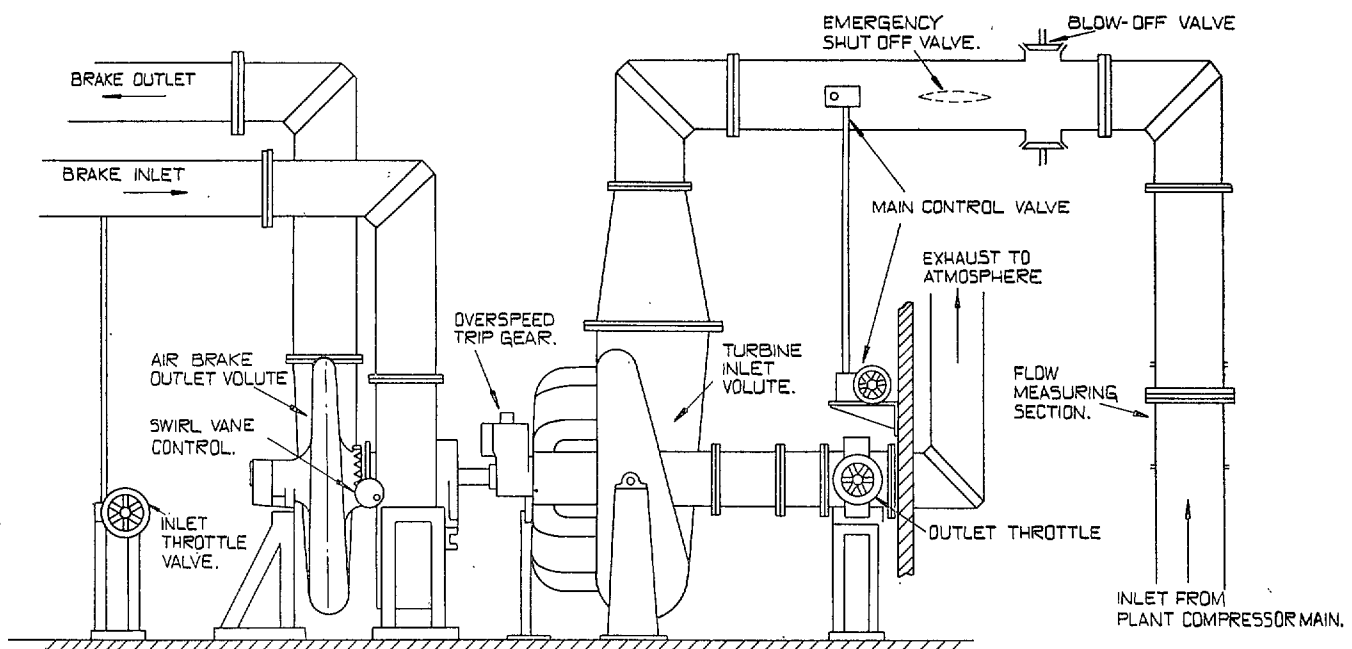
FIG. 1.   General arrangement of test equipment.
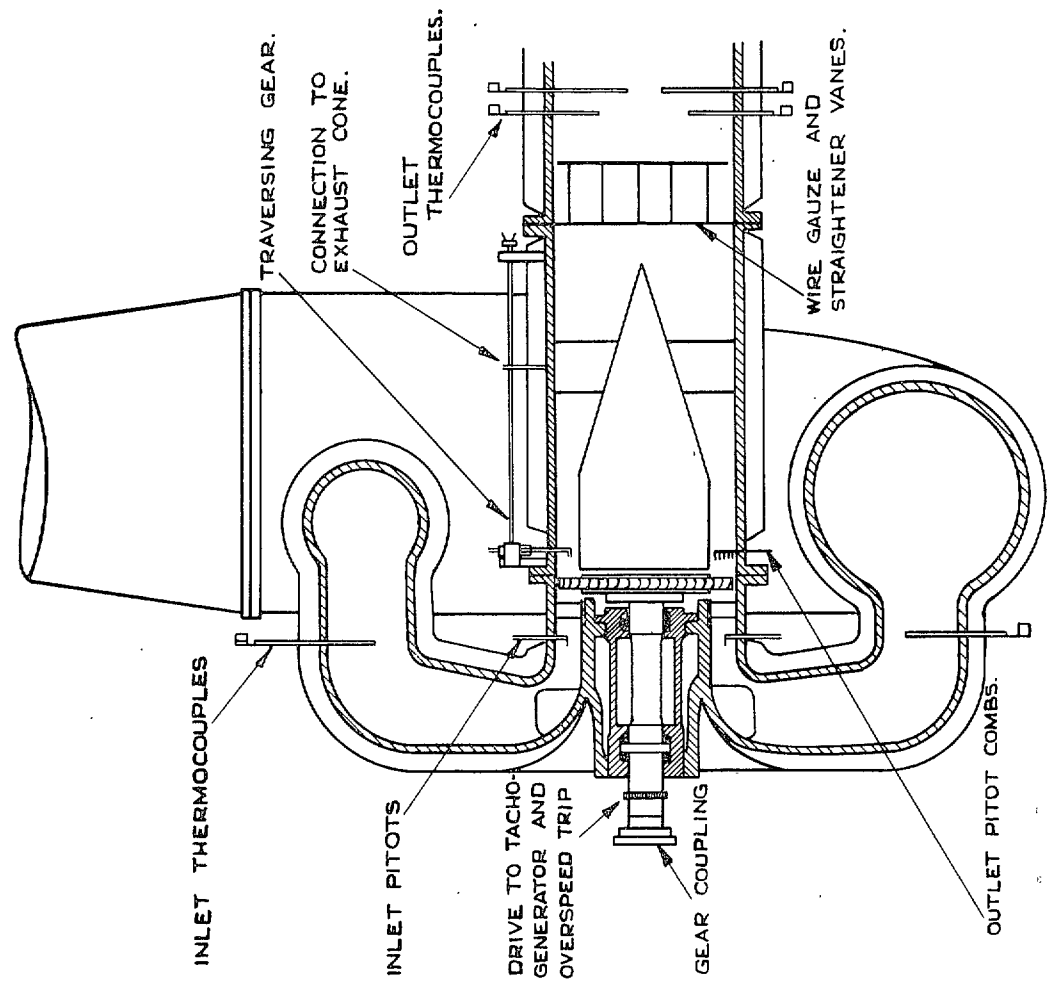
FIG. 2.   Sectional view of turbine showing test instrumentation.

8

NOZZLE BLADES.
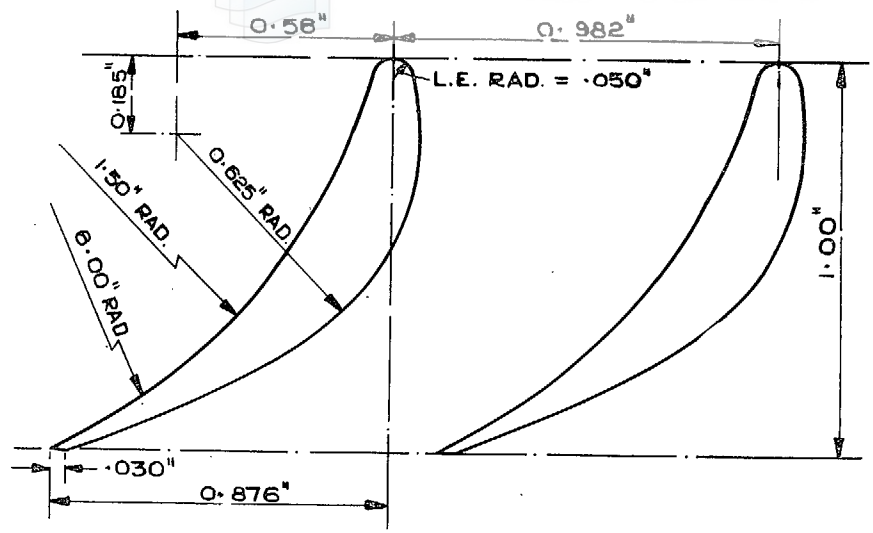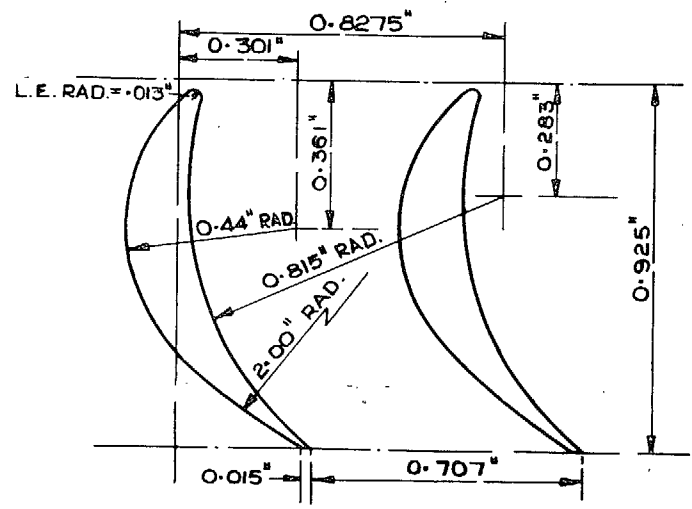
ROTOR BLADES.

FIG. 3.   Blading for single-stage turbine.   Sections at mean diameter.

X ——— CONVENTIONAL BLADES

⊙ ——— CONSTANT–SECTION, UNTWISTED BLADES
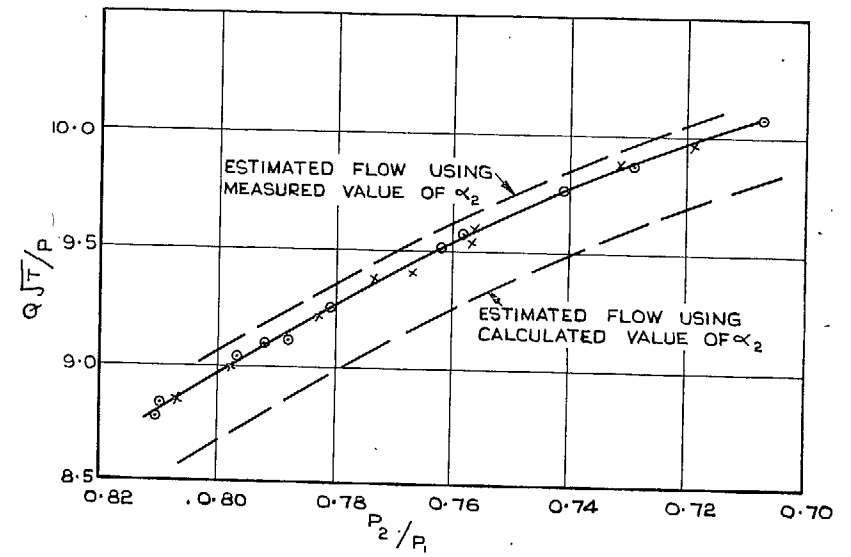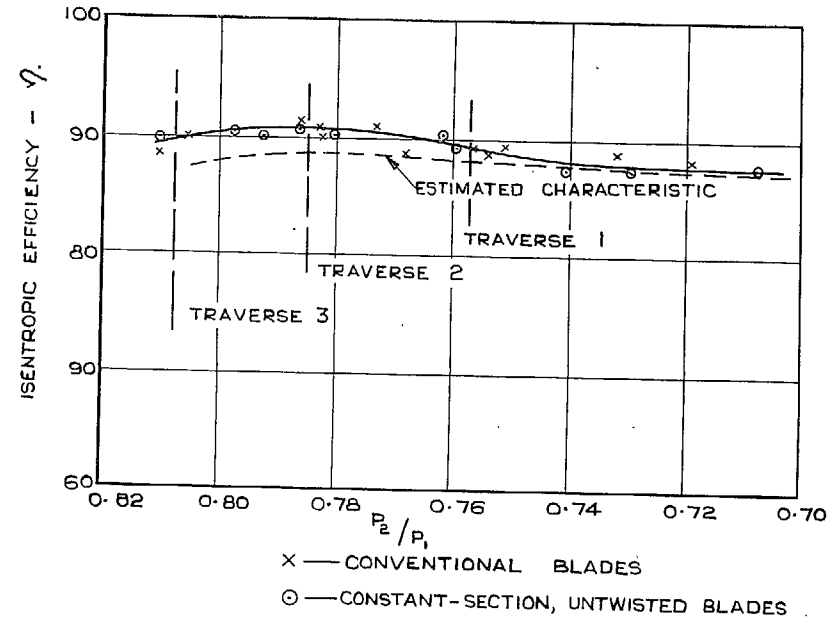
FIG. 4.   Efficiency and mass flow characteristics for twisted and
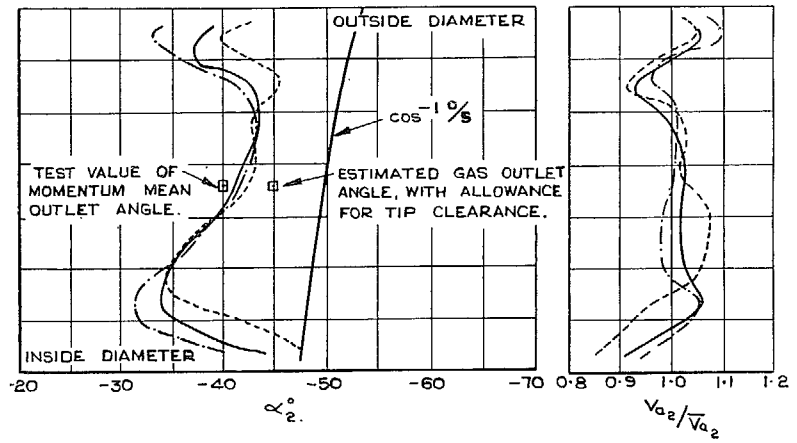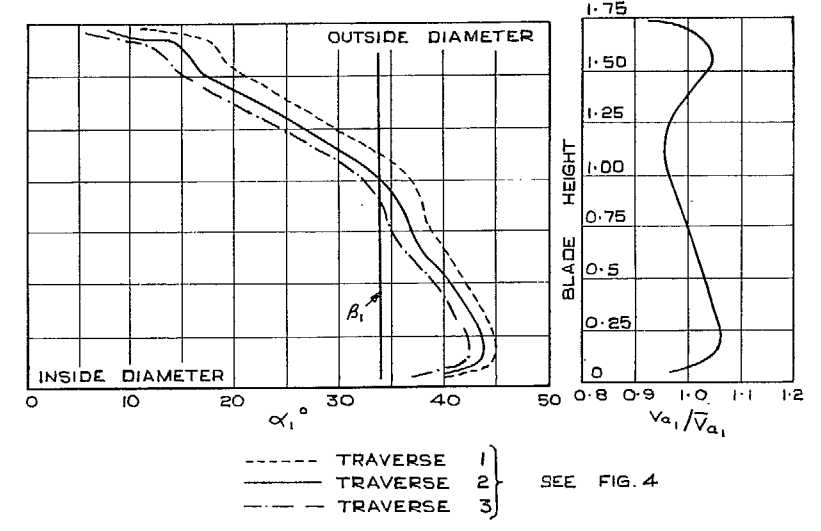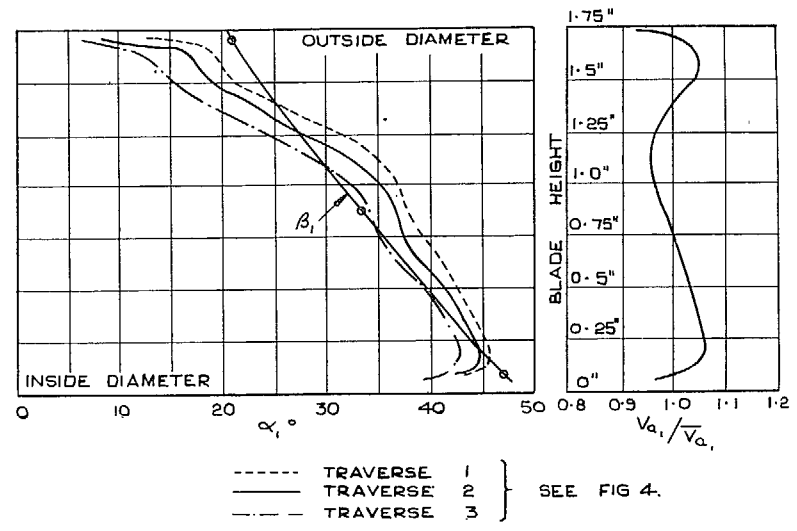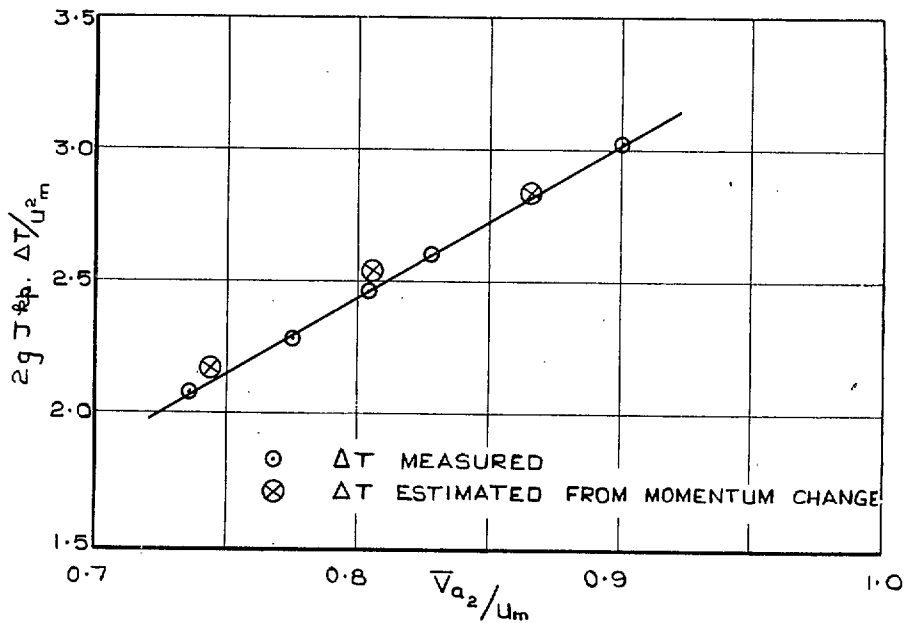untwisted rotor blades.
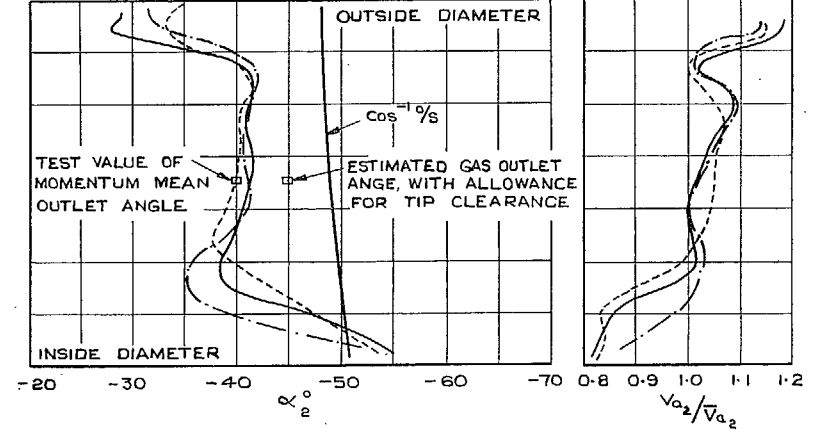
FIG. 5.   Conventional rotor.   Distributions of axial velocity
and gas angle relative to rotor blade.

FIG. 6.   Untwisted rotor.   Distributions of axial velocity
and gas angle relative to rotor blade.

10

CONVENTIONAL ROTOR BLADES.
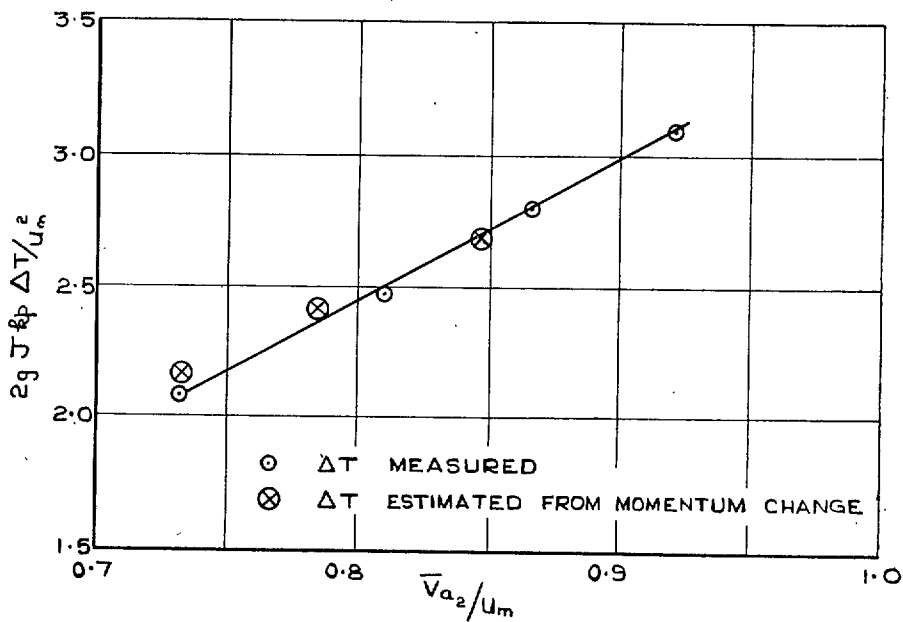

UNTWISTED ROTOR BLADES.

FIG. 7. Characteristics of mean work done coefficient with $\overline{V}_{a2}/U_m$.

Publications of the Aeronautical Research Council

ANNUAL TECHNICAL REPORTS OF THE AERONAUTICAL RESEARCH COUNCIL (BOUND VOLUMES)

1938 Vol. I. Aerodynamics General, Performance, Airscrews. 50s. (51s. 8d.)
Vol. II. Stability and Control, Flutter, Structures, Seaplanes, Wind Tunnels, Materials. 30s. (31s. 8d.)

1939 Vol. I. Aerodynamics General, Performance, Airscrews, Engines. 50s. (51s. 8d.)
Vol. II. Stability and Control, Flutter and Vibration, Instruments, Structures, Seaplanes, etc. 63s. (64s. 8d.)

1940 Aero and Hydrodynamics, Aerofoils, Airscrews, Engines, Flutter, Icing, Stability and Control, Structures, and a miscellaneous section. 50s. (51s. 8d.)

1941 Aero and Hydrodynamics, Aerofoils, Airscrews, Engines, Flutter, Stability and Control, Structures. 63s. (64s. 8d.)

1942 Vol. I. Aero and Hydrodynamics, Aerofoils, Airscrews, Engines. 75s. (76s. 8d.)
Vol. II. Noise, Parachutes, Stability and Control, Structures, Vibration, Wind Tunnels. 47s. 6d. (49s. 2d.)

1943 Vol. I. Aerodynamics, Aerofoils, Airscrews. 80s. (81s. 8d.)
Vol. II. Engines, Flutter, Materials, Parachutes, Performance, Stability and Control, Structures. 90s. (91s. 11d.)

1944 Vol. I. Aero and Hydrodynamics, Aerofoils, Aircraft, Airscrews, Controls. 84s. (86s. 9d.)
Vol. II. Flutter and Vibration, Materials, Miscellaneous, Navigation, Parachutes, Performance, Plates and Panels, Stability, Structures, Test Equipment, Wind Tunnels. 84s. (86s. 9d.)

ANNUAL REPORTS OF THE AERONAUTICAL RESEARCH COUNCIL—

1933–34	1s. 6d. (1s. 8½d.)	1937	2s. (2s. 2½d.)
1934–35	1s. 6d. (1s. 8½d.)	1938	1s. 6d. (1s. 8½d.)
April 1, 1935 to Dec. 31, 1936 4s.	(4s. 5½d.)	1939–48	3s. (3s. 3½d.)

INDEX TO ALL REPORTS AND MEMORANDA PUBLISHED IN THE ANNUAL TECHNICAL REPORTS, AND SEPARATELY—

April, 1950 – – – – – R. & M. No. 2600. 2s. 6d. (2s. 7½d.)

AUTHOR INDEX TO ALL REPORTS AND MEMORANDA OF THE AERONAUTICAL RESEARCH COUNCIL—

1909–January, 1954 – – – R. & M. No. 2570. 15s. (15s. 5½d.)

INDEXES TO THE TECHNICAL REPORTS OF THE AERONAUTICAL RESEARCH COUNCIL—

December 1, 1936 — June 30, 1939.	R. & M. No. 1850.	1s. 3d. (1s. 4½d.)
July 1, 1939 — June 30, 1945. –	R. & M. No. 1950.	1s. (1s. 1½d.)
July 1, 1945 — June 30, 1946. –	R. & M. No. 2050.	1s. (1s. 1½d.)
July 1, 1946 — December 31, 1946.	R. & M. No. 2150.	1s. 3d. (1s. 4½d.)
January 1, 1947 — June 30, 1947. –	R. & M. No. 2250.	1s. 3d. (1s. 4½d.)

PUBLISHED REPORTS AND MEMORANDA OF THE AERONAUTICAL RESEARCH COUNCIL—

Between Nos. 2251–2349. – –	R. & M. No. 2350.	1s. 9d. (1s. 10½d.)
Between Nos. 2351–2449. – –	R. & M. No. 2450.	2s. (2s. 1½d.)
Between Nos. 2451–2549. – –	R. & M. No. 2550.	2s. 6d. (2s. 7½d.)
Between Nos. 2551–2649. – –	R. & M. No. 2650.	2s. 6d. (2s. 7½d.)

Prices in brackets include postage

HER MAJESTY'S STATIONERY OFFICE